IIE Transactions (2004) **36**, 1099–1105

ISSN: 0740-817X print / 1545-8830 online
DOI: 10.1080/07408170490500672

A scale model for fitting object shapes from fixed location data

JAVIER CABRERA,[1] KWOK-LEUNG TSUI[2*] and RAVINDRA S. GOONETILLEKE[3]

[1] *Department of Statistics, 471 Hill Center, Busch Campus, Rutgers University, Piscataway, NJ 08854, USA*
E-mail: cabrera@rci.rutgers.edu
[2] *School of Industrial and Systems Engineering, Georgia Institute of Technology, Atlanta, GA 30332, USA*
E-mail: ktsui@isye.gatech.edu
[3] *Department of Industrial Engineering and Engineering Management, Hong Kong University of Science and Technology, Clear Water Bay, Kowloon, Hong Kong*
E-mail: ravindra@ust.hk

Accepted January 2004

In this paper we present a scale model for fitting an ideal shape to an object. The measurements of the object are taken corresponding to a fixed coordinate system at a set of well-defined locations on the surface of the object. We propose an algorithm to estimate the model parameters and hypothesis tests to make statistical inferences about several possible special cases of the general model. The model is tested with an example that analyzes data on the feet of people in Hong Kong.

1. Model and interpretation

Shape and size have tremendous influence when designing objects, equipment, and tools to fit people. Some consumer products can be bought in different sizes. When these different products of one commodity retain the shape but are scaled differently, they are said to be "geometrically similar". In other words, they have isometry. For example, a cube will have its length:width:height ratios the same for smaller as well as larger sizes. When one or more dimensions of a shape change disproportionately with size, that object is said to scale allometrically. Allometery has been shown to apply to people and animals (McMahon, 1975; Ross and Ward, 1981; Biewener, 1992; Brown and West, 2000; Lindstedt and Schaeffer, 2002). A similar relation is to be expected even for body parts such as feet. A person with twice the average foot length is not anticipated to have double the foot width.

The objective of our study is to understand the shape structure of an object of interest by fitting the observed data to various models. In the study, the measurements of each object are taken corresponding to a fixed coordinate system at a set of well-defined locations on the surface of the object. As the coordinate systems of various objects may differ from each other, a transformation is needed to align the observed data to the same orientation before fitting data to the object shape. Although the applications that we have in mind are for measuring two-dimensional and three-dimensional objects, it should be pointed out that the methodology presented here is general and it applies to objects in any dimension. In the remainder of this section, we will introduce the basic model and how it is related to shape data. Section 2 discusses a general algorithm for estimating the parameters of the model. Section 3 addresses statistical inference and model selection. The proposed methods are illustrated with a real-life foot shape example in Section 4.

Equation (1) gives a simple model that describes the relationship between the observed data and the ideal measurements of the fixed locations of the object:

$$\mathbf{y}_{ij} = \boldsymbol{\mu}_i + \mathbf{A}_i\mathbf{x}_j + \boldsymbol{\epsilon}_{ij}, \tag{1}$$

where $\mathbf{y}_{ij},\ j = 1, 2, \ldots, m,\ i = 1, 2, \ldots, n,$ represents the three-dimensional vector of measurements of the jth location for the ith subject. The quantities $\mathbf{x}_j,\ j = 1, 2, \ldots, m,$ are the vectors of ideal measurements at the m locations after proper scaling and alignment, which is the same for each object. The quantities $\mathbf{A}_i$ and $\boldsymbol{\mu}_i$ are the scale and translation functions that transform the ideal vector ($\mathbf{x}_j$) to a corresponding vector for the ith object ($\boldsymbol{\mu}_i + \mathbf{A}_i\mathbf{x}_j$) according to its size and coordinate system. Finally, $\boldsymbol{\epsilon}_{ij}$ represents the deviation of the actual vector measurements ($\mathbf{y}_{ij}$) from the transformed vector caused by deformation and measurement errors. As these two sources of error are related to the size of the ith object as well as the jth location of the measurement, it is assumed that $\boldsymbol{\epsilon}_{ij}$ follows a multivariate

*Corresponding author

normal distribution with zero mean and covariance matrix $\mathbf{A}_i'\boldsymbol{\Sigma}_j\mathbf{A}_i$, where $'$ denotes the matrix transpose. To interpret this covariance structure, it is helpful to consider the following transformed model:

$$\mathbf{A}_i^{-1}\mathbf{y}_{ij} = \mathbf{A}_i^{-1}\boldsymbol{\mu}_i + \mathbf{x}_j + \boldsymbol{\epsilon}_{ij}^*, \tag{2}$$

where $\boldsymbol{\epsilon}_{ij}^* = \mathbf{A}^{-1}\boldsymbol{\epsilon}_{ij}$ has a covariance matrix $\boldsymbol{\Sigma}_j$. It follows from this model that the error of the observed data after an appropriate scale transformation ($\mathbf{A}_i^{-1}$) depends only on the location of the measurement but not on the object-to-object variation, i.e., $\boldsymbol{\Sigma}_j$ depends on j only. The object-to-object variation is assumed to be proportional to the object size and is modeled by the scale function $\mathbf{A}_i$ as described by the covariance matrix of $\boldsymbol{\epsilon}_{ij}$, $\mathbf{A}_i'\boldsymbol{\Sigma}_j\mathbf{A}_i$. This type of scale variance structure is commonly used to model univariate data with variance proportional to the mean.

Note that the transformation $\mathbf{A}_i$ in model (1) involves both a rotation and scale transformation. In the problem of modeling part geometry in manufacturing applications, it is common to consider only the rotation without the scale transformation. However, model (1) proposed here allows more flexible shape structures in part geometric modeling. This issue will be addressed separately.

2. Algorithm

The algorithm that we present here can be used for measuring objects in any dimension. The basic steps are general; although the details of the calculations herein are for the two-dimensional case, they can be adapted to three or more dimensions with only a few changes.

Under normality, the Maximum Likelihood Estimators (MLE's) for the model parameters are obtained by minimizing the function:

$$\sum_{i=1}^{n}\sum_{j=1}^{m}\{\mathbf{B}_i\mathbf{y}_{ij} - \boldsymbol{\nu}_i - \mathbf{x}_j\}'\boldsymbol{\Sigma}_j^{-1}\{\mathbf{B}_i\mathbf{y}_{ij} - \boldsymbol{\nu}_i - \mathbf{x}_j\}, \tag{3}$$

where $\boldsymbol{\nu}_i = \mathbf{B}_i\boldsymbol{\mu}_i$ is just a reparameterization of the $\boldsymbol{\mu}_i$s and $\mathbf{B}_i = \mathbf{A}_i^{-1}$. The quantity $\mathbf{A}_i$ is the product of an orthogonal matrix $\mathbf{H}_i$ times a diagonal matrix $\mathbf{E}_i$. Its inverse may be written as $\mathbf{B}_i = \mathbf{D}_i\mathbf{H}_i'$, where the diagonal matrix $\mathbf{D}_i = \mathbf{E}_i^{-1}$.

Equation (3) contains four groups of parameters. The first three groups are $\{\mathbf{D}_i\}$, $\{\mathbf{H}_i\}$ and $\{\boldsymbol{\nu}_i\}$, which correspond to the scale, rotation, and orientation of each individual object. The fourth group contains the remaining parameters of the location and scatter at each marker, $\{\mathbf{x}_j\}$ and $\{\boldsymbol{\Sigma}_j\}$. Our algorithm consists of iterations that at each step estimate one of the four groups of parameters by keeping the other three fixed.

In order to make the model identifiable we need to set up some constraints on the location and dispersion of the standard object. The center of the standard object should be set to zero, and the scale should be set to the average scale of the observed sample. This is calculated at the initial step.

For notational convenience we may replace $\boldsymbol{\Sigma}_j^{-1}$ by its Cholesky decomposition $\mathbf{W}_j'\mathbf{W}_j$ in Equation (3), which results in:

$$\sum_{i=1}^{n}\sum_{j=1}^{m}\{\mathbf{W}_j(\mathbf{B}_i\mathbf{y}_{ij} - \boldsymbol{\nu}_i - \mathbf{x}_j)\}'\{\mathbf{W}_j(\mathbf{B}_i\mathbf{y}_{ij} - \boldsymbol{\nu}_i - \mathbf{x}_j)\}.$$

Differentiating with respect to $\boldsymbol{\nu}_i$ we get:

$$\sum_{j=1}^{m}\mathbf{W}_j'\mathbf{W}_j(\mathbf{B}_i\mathbf{y}_{ij} - \boldsymbol{\nu}_i - \mathbf{x}_j) = 0, \tag{4}$$

which suggests the constraint $\sum_{j=1}^{m}\boldsymbol{\Sigma}_j^{-1}\mathbf{x}_j = 0$ for centering the object at zero. Since the variances of the estimated markers of the standard object are unequal, the center of the points is calculated as a weighted average with weights inversely proportional to the variances.

Since we have four groups of parameters, the algorithm consists in the same number of steps. At each step we estimate one of the four groups assuming that the other three are known and using our current estimates as if they were the true values. An appealing feature of the algorithm is that it can be implemented easily in the S language, since each step can be evaluated using existing Splus (Chambers and Hastie, 1992) functions for model fitting or matrix operations. A good description of the numerical methods that are applied here can be found in Thisted (1985).

Algorithm

Step 1. Estimate $\{\boldsymbol{\nu}_i\}$.
From Equation (4) and using the constraint on the $\mathbf{x}_j'$s we derive the estimator for $\{\boldsymbol{\nu}_i\}$:

$$\hat{\boldsymbol{\nu}}_i = \left\{\sum_{j=1}^{m}\boldsymbol{\Sigma}_j^{-1}\right\}^{-1}\sum_{j=1}^{m}\boldsymbol{\Sigma}_j^{-1}\mathbf{B}_i\mathbf{y}_{ij}.$$

Step 2. Estimate $\{\mathbf{D}_i\}$.
Since $\mathbf{D}_i$ is a diagonal matrix we denote its nonzero elements as d_{i1} and d_{i2}. The same applies to the upper triangular matrix $\mathbf{W}_j$ whose elements are denoted by w_{j1}, w_{j2}, and w_{j3}. The orthogonal matrix $\mathbf{H}_i$ is given by:

$$\begin{pmatrix}\cos(\theta_i) & \sin(\theta_i)\\ -\sin(\theta_i) & \cos(\theta_i)\end{pmatrix},$$

where θ_i represents the angle of rotation.
From Equation (3), in order to estimate $\mathbf{D}_i$ we need to minimize:

$$\sum_{j=1}^{m}\{\mathbf{W}_j\mathbf{D}_i\mathbf{H}_i'\mathbf{y}_{ij} - \mathbf{W}_j(\boldsymbol{\nu}_i + \mathbf{x}_j)\}'\{\mathbf{W}_j\mathbf{D}_i\mathbf{H}_i'\mathbf{y}_{ij} - \mathbf{W}_j(\boldsymbol{\nu}_i + \mathbf{x}_j)\}. \tag{5}$$

Let us write $\mathbf{u}_{ij} = \mathbf{W}_j(\boldsymbol{\nu}_i + \mathbf{x}_j)$ and $\mathbf{v}_{ij} = \mathbf{H}_i'\mathbf{y}_{ij}$; note that $\mathbf{u}_{ij}$ and $\mathbf{v}_{ij}$ are two-dimensional vectors. Then the above sum is equal to:

$$\sum_{j=1}^{m}[\{u_{ij1} - w_{j1}\mathbf{v}_{ij1}d_{i1} - w_{j2}\mathbf{v}_{ij2}d_{i2}\}^2 + \{u_{ij2} - w_{j3}\mathbf{v}_{ij2}d_{i2}\}^2].$$

Thus, the estimator of $\mathbf{D}_i$ is obtained by least squares regression.

Step 3. Estimate $\{\mathbf{H}_i\}$.
Since $\mathbf{H}_i$ depends on a parameter θ_i in a nonlinear way, it is not possible to linearize it as we did with the other parameters. To estimate θ_i we do a one-dimensional optimization of Equation (5). This is repeated for each i until we obtain the estimators of all the $\mathbf{H}_i$'s. In our implementation we used an optimization function in Splus.

Steps 4 and 5. Estimate $\{\mathbf{x}_j\}$ and $\{\boldsymbol{\Sigma}_j\}$.
When the $\boldsymbol{\nu}_i$, $\mathbf{D}_i$ and $\mathbf{H}_i$ are known it follows from Equation (3) that $\mathbf{x}_j$ and $\boldsymbol{\Sigma}_j$ are the mean and variance-covariance matrix of the points $\{\mathbf{D}_i\mathbf{H}_i'\mathbf{y}_{ij} - \boldsymbol{\nu}_i\}_{i=1}^{n}$, i.e.:

$$\mathbf{x}_j = \frac{1}{n}\sum_{i=1}^{n}(\mathbf{D}_i\mathbf{H}_i'\mathbf{y}_{ij} - \boldsymbol{\nu}_i)$$

and

$$\boldsymbol{\Sigma}_j = \frac{1}{n}\sum_{i=1}^{n}(\mathbf{D}_i\mathbf{H}_i'\mathbf{y}_{ij} - \boldsymbol{\nu}_i)(\mathbf{D}_i\mathbf{H}_i'\mathbf{y}_{ij} - \boldsymbol{\nu}_i)'.$$

Then apply the constraints to the obtained estimators $\{\mathbf{x}_j\}$ and $\{\boldsymbol{\Sigma}_j\}$ by the iterative assignment:

$$\mathbf{x}_j = \mathbf{x}_j - \left\{\sum_{l=1}^{m}\boldsymbol{\Sigma}_l^{-1}\right\}^{-1}\sum_{l=1}^{m}\boldsymbol{\Sigma}_l^{-1}x_l,$$

where $\boldsymbol{\Sigma}_0$ is the initial average of the variance-covariance matrices at each marking.

We do not have a formal proof of convergence for this algorithm. However, one attractive property of the algorithm is that all steps except (perhaps) for the last constraint on Step 5 will improve the likelihood. In addition, we have convincing empirical evidence, from all the examples we ran under many choices of initial conditions, in which the algorithm always converged to what appears to be the MLE.

3. Statistical inference

In Section 1 we introduced a general model that describes the relationship between the observed data measured at the fixed markers of the object. In some cases, a more-restricted model may be adequate to describe the relationship and provide interesting interpretations. Below we will establish a sequence of restricted models and the corresponding methods for identifying the appropriate model.

The general model and the natural starting point for the model sequence is given in Equation (3). As described the $\mathbf{A}$'s described in Section 2, the transformation $\mathbf{A}_i$ in Equation (3) is the product of an orthogonal matrix $\mathbf{H}_i$ with rotation angle θ_i and a "general" diagonal matrix $\mathbf{E}_i$ with diagonal elements $1/d_{i1}$ and $1/d_{i2}$,

$$\mathbf{E}_i = \begin{pmatrix} 1/d_{i1} & 0 \\ 0 & 1/d_{i2} \end{pmatrix}. \tag{6}$$

By adding restrictions to the matrix $\mathbf{E}_i$, we propose the following three restricted models:

$$\mathbf{E}_i = \begin{pmatrix} 1/d_i & 0 \\ 0 & 1/d_i \end{pmatrix}, \tag{7}$$

$$\mathbf{E}_i = \begin{pmatrix} 1/d_1 & 0 \\ 0 & 1/d_2 \end{pmatrix}, \tag{8}$$

$$\mathbf{E}_i = \begin{pmatrix} 1 & 0 \\ 0 & 1 \end{pmatrix}. \tag{9}$$

Each of the three restricted models has its own interpretation. As matrix $\mathbf{E}_i$ measures the size effect of the transformation, the general model (6) implies that the size effect is different for each coordinate as well as for each individual ith object. Model (7) implies that the size effect is the same for each coordinate but different for each individual object. Model (8) implies that the size effect is different for each coordinate but the same for each individual object. Finally, model (9) implies that the size effect is the same for each coordinate as well as for each individual object. Note that this last model is the same as the usual model of the localization problem in geometry modeling where only translation and rotation are allowed.

For fitting the restricted models to the data, the same algorithm described in Section 3 can be used by adding the restrictions on the matrix $\mathbf{E}_i$. The only part of the algorithm that changes is the estimation of the $\mathbf{E}_i$s in Step 2.

As the fitting method is based on MLE, the likelihood ratio test for testing hypotheses (Bickel and Doksum, 1977) can be used to identify the appropriate model. Suppose the null and alternative hypotheses are:

H_0: *The correct model is model p* or
H_A: *A better model is model q*.

It is assumed that model p is a restricted version of model q. Suppose the number of unknown parameters in models p and q are m_p and m_q respectively. Then under the null hypothesis H_0, the test statistic $T_0 = -2\log(\lambda)$ converges to a chi-square distribution with $(m_q - m_p)$ degrees of freedom, where λ is the ratio of the likelihood for model p over the likelihood for model q. In the cases of models (6) and (7) the conditions for the asymptotic distribution are not met since the number of parameters goes to infinity with the sample size. The ratio between the number of parameters and the number of observations is small but does not go to zero. Although we do not have a proof that for these models the asymptotic distribution of the likelihood ratio statistic is chi-square, we conducted some simulations for our specific configuration that showed that the approximation was adequate.

The likelihoods are calculated using the normal distribution assumptions for the corresponding model.

The covariance matrix for an observation of the jth point from the ith foot is $\mathbf{A}_i'\boldsymbol{\Sigma}_j\mathbf{A}_i$; for each model, since we have estimates of $\mathbf{A}_i$ and $\boldsymbol{\Sigma}_j$, the covariance matrix can also be estimated by, say, $\hat{\boldsymbol{\Sigma}}_{q,ij}$ for the full model and $\hat{\boldsymbol{\Sigma}}_{p,ij}$ for the restricted one. The log-likelihood for the full model (model q) is

$$\log(\text{lik}_q) = \sum_{i,j}[-\log(2\pi) - \log(|\hat{\boldsymbol{\Sigma}}_{q,ij}|)] - \frac{1}{2}\sum_{i,j}(\mathbf{y}_{ij} - \hat{\mathbf{y}}_{q,ij})'\hat{\boldsymbol{\Sigma}}_{q,ij}^{-1}(\mathbf{y}_{ij} - \hat{\mathbf{y}}_{q,ij}),$$

where $|\cdot|$ is the determinant of the matrix and $\hat{\mathbf{y}}_{q,ij}$ is the estimate of the jth point from the ith foot under the full model. The log-likelihood for the restricted model is the same with q replaced by p. After simplification the log-likelihood ratio test statistic can be written as:

$$\begin{aligned} T_0 &= -2\log(\lambda), \\ &= \sum_{i,j} 2\log(\det|\hat{\boldsymbol{\Sigma}}_{p,ij}|) + \sum_{i,j}(\mathbf{y}_{ij} - \hat{\mathbf{y}}_{p,ij})'\hat{\boldsymbol{\Sigma}}_{p,ij}^{-1}(\mathbf{y}_{ij} - \hat{\mathbf{y}}_{p,ij}), \\ &\quad - \sum_{i,j} 2\log(\det|\hat{\boldsymbol{\Sigma}}_{q,ij}|) - \sum_{i,j}(\mathbf{y}_{ij} - \hat{\mathbf{y}}_{q,ij})'\hat{\boldsymbol{\Sigma}}_{q,ij}^{-1} \\ &\quad \times (\mathbf{y}_{ij} - \hat{\mathbf{y}}_{q,ij}). \end{aligned}$$

Thus, an approximate test is to reject the null hypothesis H_0 versus H_A at a significance level of α when $T_0 > \chi^2_{\alpha,m_q-m_p}$.

Two sequences of models can be established to identify the appropriate model. The first sequence is to test model (6) against model (7); if model (6) is rejected, we test model (7) against model (8). The second sequence is to test model (6) against model (8); if model (6) is rejected, we test model (8) against model (9). Meaningful interpretations can be drawn based on the sequence and the interpretations of the models involved. In the next section a real-life case involving the investigation of human foot geometry will be used to illustrate the model identification method as well as the interpretations described above.

4. A Hong Kong foot example

The data were obtained by the Human Performance Laboratory at the Hong Kong University of Science and Technology. A random sample of 50 male subjects between 18 and 22 years old was taken and each individual's left foot was measured. The measurement procedure for each foot consisted of locating 64 points on the foot surface and measuring the coordinates of each in three-dimensional space. These 64 points were chosen to give an accurate description of the foot shape. A more detailed description of the experiment can be found in Goonetilleke *et al.* (1997).

The data consist of 50 arrays of dimension 3×64, each representing an individual foot. For simplicity, we will show here only the two-dimensional projections of the foot into the reference xy-plane. In the remainder of the paper we will use the term "foot" to refer to each subject datum, that is, to a set of 64 two-dimensional points.

The data were pre-processed by centering each foot at the origin and aligning the first principal component of each foot to the x-axis (and it follows that the second principal component is aligned to the y-axis). These centering and rotation operations provide a good starting point for the

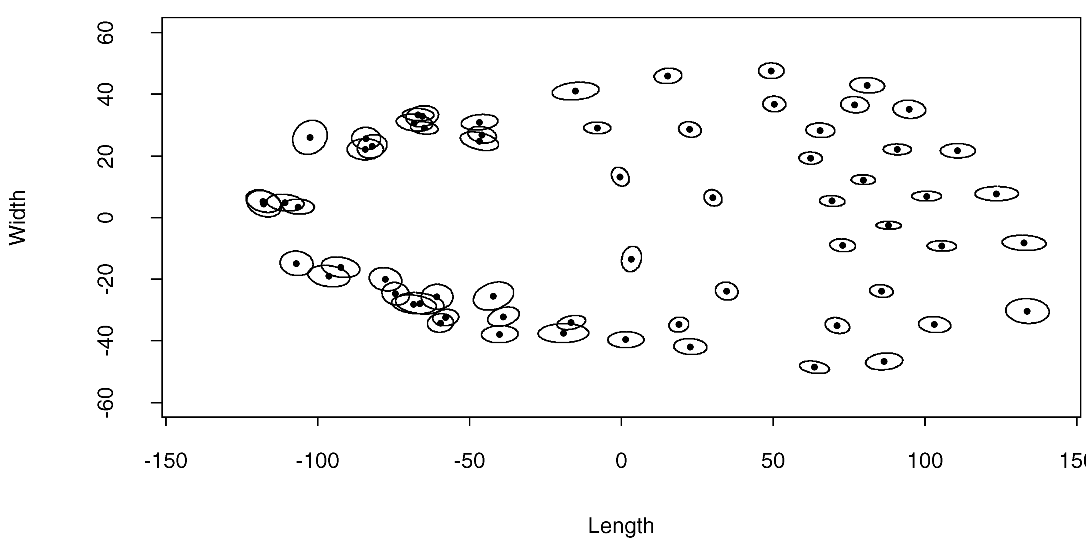

Fig. 1. Error variance structure at each mark.

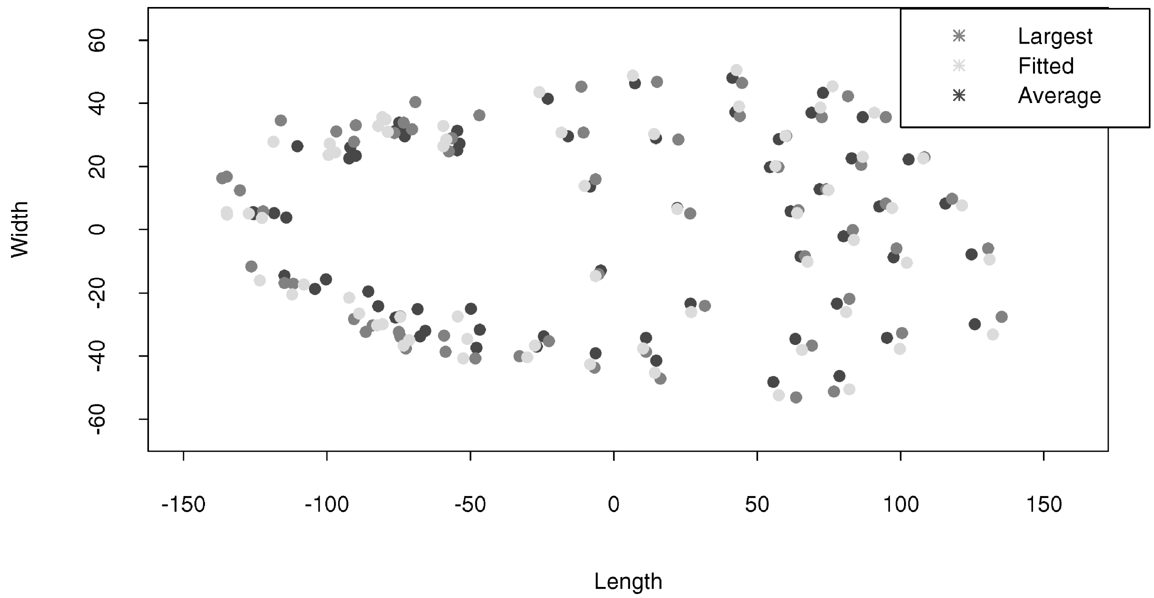

Fig. 2. Comparison of the largest foot on the sample with the fitted foot and the ideal foot.

algorithm in Section 2 since it should be reasonably close to the optimal solution. Figure 1 shows the sample average and sample variances for each of the 64 landmarks on the foot. This picture is not too different from the one we obtain if we calculate the sample variances from the residuals of the fitted model. The widespread variation in the ellipses is a strong indication that the distributions at the 64 sites have unequal variance-covariance matrices, and it justifies this aspect of the model.

The estimation procedure was performed and the algorithm converged after 10 to 20 iterations depending on the model. The starting point for the algorithm was obtained from the initial positions of the data, by calculating the average foot and the initial covariance matrices at each site. In addition, the algorithm was tested at five different starting points by adding random error and rescaling the initial average foot and sample covariances; and the algorithm converged to the same solution with only one or two more iterations.

Figures 2 and 3 show the largest and smallest feet in the sample with their corresponding fitted values and the fitted ideal foot.

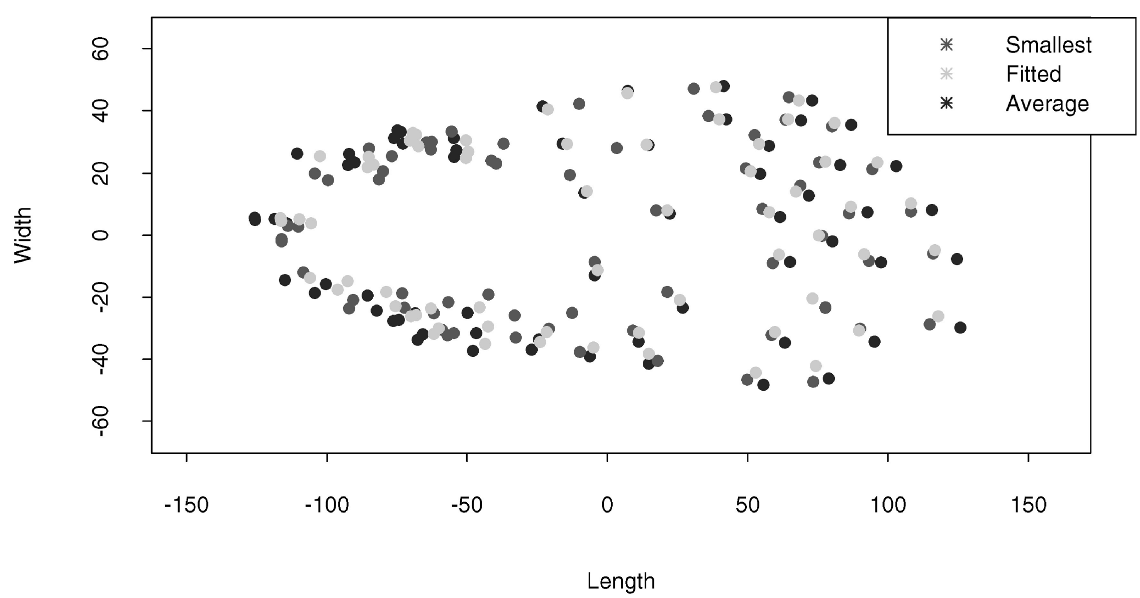

Fig. 3. Comparison of the smallest foot on the sample with the fitted foot and the ideal foot.

Table 1. Likelihood ratio tests for comparing models (6)–(9)

Comparison	T_0	*d.f.*	p-*value*
Model (6) vs. Model (7)	695	50	0.000
Model (7) vs. Model (9)	4829	50	0.000
Model (6) vs. Model (8)	5522	98	0.000
Model (8) vs. Model (9)	2.88	2	0.237

In addition to estimating the general model we also calculated the MLEs for the alternative models in Section 3. The algorithm from Section 2 was used with the necessary modifications to accommodate the restrictions in the parameters imposed by the models. In order to select the most appropriate model we performed the sequence of likelihood ratio tests proposed in Section 3. The test statistic $T_0 = -2\log(\lambda)$ was calculated for the four relevant comparisons. Table 1 shows the results for the various hypotheses and their corresponding statistics. The first three hypotheses were rejected with p values close to zero. The last hypothesis was not rejected with a p-value of 0.237.

Table 1 provides strong evidence in favor of model (6) which justifies: (i) using different scale parameters for different feet; and (ii) using two different scale parameters for the width and length at each foot. All comparisons are strongly significant except for that of model (8) against model (9), which indicates that when the scale parameters are restricted to be the same for each foot, it does not matter whether or not the scale parameters for the width and length are different. In summary, model (6) is the best model, and the other models become less and less adequate as the number of parameters is reduced.

As previously noted Figs. 2 and 3 show the largest and smallest feet in the sample with their corresponding fitted values and the average fitted foot after appropriate centering. Figure 2 shows that the points of the average foot are circumscribed by the observed points of the largest foot and their corresponding fitted values. According to model (1), the deviation of the average fitted points from the individual fitted points can be explained by the different scale parameter for each foot as well as the different parameters for the width and length. There is clearly a proportional pattern between these two sets of points. The deviations of the actual observed points from the individual fitted points can be explained by the deformation and measurement errors. Figure 3 shows that the observed points of the smallest foot and their corresponding fitted values are circumscribed by the points of the average foot. Similarly, the same kind of deviation patterns exist.

Figure 4 shows the histogram of the estimated angle of rotation, which varies between -1° and 1° approximately. This is a good indication that the principal components initial estimate does a good job at aligning the foot.

Figure 5 gives a scatter plot of the length factor against the width factor, and although they are correlated, the correlation is very weak, thus stressing the improvement of model (6) compared to model (7). These figures clearly show that the fitted model (6) is a good improvement over the other models. Nevertheless, there are some small systematic differences between the fitted feet and the data. It appears that the scale in the front of the foot may not be consistent with the scale in the back or the middle. This can be seen by the deviations between the observed points and the individual fitted points. In particular, there seem to be differences in the goodness of the fit between the three parts of the foot: front, back, and center. It will be interesting to test an extended version of model (6) in which the scale parameters for the width and length are different at the three parts of the foot.

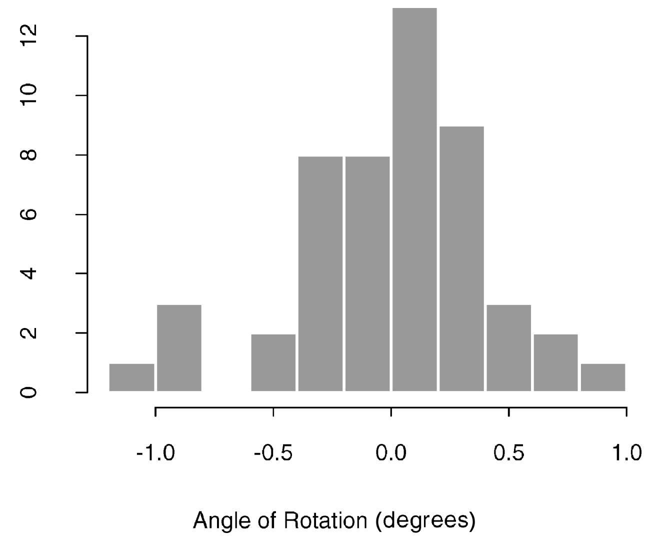

Fig. 4. Histogram of the angles of rotation of the 64 points.

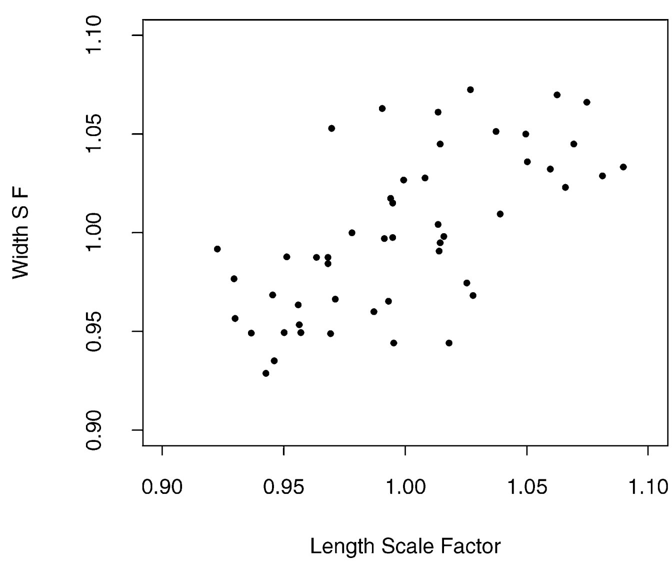

Fig. 5. Scatter plot of foot width against the foot length relative to the ideal foot.

Finally, although the performance of the model in this example is quite satisfactory, we feel that more can eventually be done. Further modeling that goes beyond the scope of this paper is needed and is ongoing.

Acknowledgements

J. Cabrera was supported in part by National Science Foundation Grant IRI-9530546 96. R. S. Goonetilleke and K.-L. Tsui were supported in part by RGC Grants HKUST 798/96E.

References

Bickel, P.J. and Doksum, K.A. (1977) *Mathematical Statistics*, Holden-Day, New York, NY.

Biewener, A.A. (1992) *Biomechanics—Structures and Systems. A Practical Approach*, Oxford University Press, London, UK.

Brown, J.H. and West, G.B. (eds.) (2000) *Scaling in Biology,* Oxford University Press, New York, NY.

Chambers, J.M. and Hastie, T.J. (1992) *Statistical Models in S*, Wadsworth, New York.

Goonetilleke, R.S., Ho, C.F. and So, H.Y. (1997) Foot sizing beyond the 2-D Brannock method. *Annual Journal of IIE* (*HK*), 28–31.

Lindstedt, L. and Schaeffer, P.J. (2002) Use of allometry in predicting anatomical and physiological parameters of mammals. *Laboratory Animals*, **36**(1), 1–19.

McMahon, T.A. (1975) Using body size to understand the structural design of animals: quadrupedal locomotion. *Journal of Applied Physiology*, **39**(4), 619–627.

Ross, W.D. and Ward, R. (1981) *Sexual Dimorphism and Human Proportionality: Sexual Dimorphism in Homo Sapiens*, Praeger, New York, NY, ch. 7.

Thisted, R.A. (1985) *Elements of Statistical Computing,* Chapman and Hall, New York, NY.

Biographies

Javier Cabrera is on the faculty of the Department of Statistics at Rutgers University. He teaches and conducts research in statistical computing and graphics, computer vision, and directional data analysis. He is a coauthor of the texts *Statistical Consulting* (with Andrew McDougall) and *Exploration and Analysis of DNA Microarray and Protein Array Data* (with Dhammika Amaratunga). He received his Ph.D. from Princeton and was a Fulbright Scholar.

Kwok-Leung Tsui is a Professor in the School of Industrial and Systems Engineering at the Georgia Institute of Technology. He is well known for his work in statistical methods for quality and productivity improvement. His current research interests include robust design and the Taguchi method, experimental design, statistical process control, data mining, bioinformatics, supply chain management, design and modeling of computer experiments, and design and analysis of coordinate measuring machine experiments. He received his Ph.D. in Statistics from the University of Wisconsin at Madison in 1986. He is a US representative of the ISO Technical Committee in Statistical Methods. He was the chair-elect and chair of the Quality, Statistics, and Reliability Section for INFORMS during 1999–2000.

Ravindra S. Goonetilleke is an Associate Professor in the Department of Industrial Engineering and Engineering Management at Hong Kong University of Science and Technology. His primary research interests lie in modelling human performance and the development of user-friendly products and computer systems, e.g., footwear design and development, mental model development, and applications of sensation and perception theories to product development. He earned an MS in Aerospace Engineering (1985) from the Georgia Institute of Technology in Atlanta, an MS in Industrial Engineering (1983) and a PhD in Human Factors Engineering (1990) from the State University of New York at Buffalo. He was a Fulbright Scholar while pursuing postgraduate studies.